Sensors and Materials, Vol. 38, No. 6 (2026) 3653–3664
MYU Tokyo

S & M 4526

Sensor-integrated Deep Learning Model for Elderly Care Coordination in Industrial Transition Regions of China: Architecture, Calibration, and Validation

Yue Geng,[1] Fuling Wang,[1*] and Weiyuan Yang[2]

[1]Shenyang Institute of Science and Technology, Shenyang 110167, China
[2]Shenyang City University, Shenyang 110112, China

(Received May 11, 2026; accepted June 23, 2026)

Keywords: elderly health care, coupling coordination degree, LSTM-DNN model, sensor-based healthcare, industrial transition region, healthcare integration

Rapid population aging and industrial restructuring make coordination between public elderly care services (PECS) and the elderly care industry (ECI) critical for improving healthcare outcomes in transition regions. In this study, a modified quadruple-subject coordination model (government–market–family–unit) was introduced to develop a sensor-integrated long short-term memory (LSTM)–deep neural network (DNN) model and evaluate the coupling coordination degree (CCD) of elderly healthcare systems. Multi-modal sensor data, including the global navigation satellite system (GNSS) parsing of National Marine Electronics Association (NMEA) 0183 Standard, the 2.4 GHz active RF identification tracking of electronic product code strings, mattress-embedded piezoresistive force sensors, dual-beam passive infrared (PIR) arrays, and 13.56 MHz near-field communication (NFC) handshakes, was collected across 14 prefecture-level cities in Liaoning Province, China. To fuse asynchronous data, a two-stage synchronization protocol employing rolling median filtering and bucket-aggregation grids was implemented before conducting sequence learning. Liaoning's CCD increased from 0.54 in 2018 (barely coordinated) to 0.79 in 2023 (moderately coordinated), progressing through preliminary, policy-driven, and optimization stages. The hybrid model eliminated gradient instability, reducing the root mean square error by 29.3% and achieving an R^2 of 0.923 compared with models lacking physical sensing layers. Governance constraints were identified, including urban–rural resource imbalance and a 1.2-year policy execution latency. By integrating explicit time-delay variables and Kalman filtering and adaptive drift correction, the developed model provides a reproducible, scalable approach for sensor-based healthcare governance evaluation in industrial transition regions.

1. Introduction

Research on aging has traditionally been conducted by using active aging theory[(1)] and the long-term care triangle model.[(2)] These frameworks emphasize the roles of market and family as

*Corresponding author: e-mail: 13840109011@163.com
https://doi.org/10.18494/SAM6408

ISSN 0914-4935

actors in elderly care but often overlook the transformative potential of emerging technologies, particularly sensor technology, in facilitating multi-party interaction and coordination.(3) Moreover, the industrial dimension of aging, which necessitates digital data integration to capture the socioeconomic effects of demographic change, has not been fully considered.

Coupling coordination degree (CCD) evaluation methods, widely applied in aging research, combine the CCD model with entropy weight and the technique for order of preference by similarity to ideal solution. Although useful, the methods are limited in capturing the temporal dynamics inherent in rapidly evolving demographic and industrial transitions.(4) To overcome this limitation, researchers have introduced deep learning models such as long short-term memory (LSTM) and deep neural networks (DNNs). However, these models are primarily established on the basis of the data from statistical yearbooks, which fail to reflect real-time demographic shifts and industrial impacts.(5) Furthermore, deep learning models in elderly care have been under-optimized for heterogeneous sensing data, where noise and variability significantly affect model fidelity.(6)

Sensor technology has demonstrated strong effectiveness in local health monitoring and IoT-based facility tracking.(7,8) However, most traditional applications remain confined to isolated, single-scenario deployments that function independently of broader governance frameworks.(9) The major constraint is not the absence of standardized deployment or calibration protocols,(10) but the methodological challenge of translating physical sensor telemetry into systemic administrative logic. For industrial transition regions, where localized ambient monitoring must be scaled into macro-level evaluation metrics, a coordination model becomes essential.(9) These limitations reveal three critical gaps. The first is a theoretical gap, as existing models remain unit-centric and overlook the industrial legacy and its implications when examined through a sensing perspective. The second is a methodological gap, since conventional CCD evaluation approaches lack a dedicated sensing layer capable of integrating multi-modal data streams. The third is an empirical gap, as the effect of specific sensor parameters such as precision and response latency on regional health outcomes remains insufficiently explored.

Therefore, we developed a health services coordination system tailored to industrial transition regions. The system integrates heterogeneous sensor data into a CCD evaluation framework and employs a sensor-enhanced LSTM-DNN model to identify evidence-based policies for improving elderly care service delivery. To achieve this, sensor data were collected across 14 prefecture-level cities in Liaoning Province, China, and a sensor-integrated evaluation model was constructed to bridge micro-level telemetry with macro-level governance outcomes.

2. Methods

2.1 Study area

Liaoning Province, located in Northeast China, represents an industrial transition region facing rapid demographic challenges. As one of China's traditional industrial bases, Liaoning has long relied on heavy industries such as coal mining, steel production, and machinery manufacturing. However, the province has undergone significant restructuring toward service-

oriented and high-tech sectors, creating both opportunities and vulnerabilities in its social and economic systems. Demographically, Liaoning is the most severely aging province in China.

In 2023, the proportion of residents aged 60 and above reached 29.4% (12.3 million), while those aged 65 and above accounted for 21.1%—figures substantially higher than the national averages.[1] This aging-before-affluence phenomenon, coupled with industrial restructuring, has intensified the demand for coordinated elderly care services. The coexistence of rapid demographic change and economic transition makes Liaoning an ideal setting to investigate how sensor-based frameworks can enhance healthcare coordination in aging societies.

Structurally, two challenges are found in the province's elderly care system. First, the public elderly care services (PECS), which form the backbone of the social security system, remain insufficiently developed to meet the diverse needs of the population. Second, the elderly care industry (ECI) has not yet been upgraded to align with these demands, resulting in persistent coordination failures. These are reflected in a 37% urban–rural gap in facility coverage and a policy coordination rate of only 18%. Moreover, the absence of a unified, real-time sensing infrastructure in industrial zones has created blind spots in service utilization and resource allocation.[9]

2.2 Data acquisition

This study was conducted in 14 prefecture-level cities in Liaoning Province, China (Shenyang, Dalian, Anshan, Fushun, Benxi, Dandong, Jinzhou, Yingkou, Fuxin, Liaoyang, Panjin, Tieling, Chaoyang, and Huludao), which have undergone significant industrial transition. Data were obtained from 2018 to 2023 by integrating official statistical records with high-fidelity sensor data. The sensor deployment network encompassed 30 elderly care institutions, 50 urban and rural communities, and 1,000 elderly participants. To ensure the robustness of the governance sensing network,[11] participants were recruited with consideration of health status, age, and residential location. Five sensors were deployed to transform localized, event-triggered behaviors into synchronized indicators.

- Spatial mapping: global positioning system (GPS) modules were used to generate National Marine Electronics Association 0183 Standard (global positioning recommended minimum specific global navigation satellite system data) at a sampling frequency of 0.1 Hz. Latitude, longitude, and ground speed readings (positioning error $\leq$ 5 m under calibrated outdoor conditions) were transmitted via low-power wide-area network protocols to local servers. These data were processed into regional mobility trajectories, which were then aggregated to calculate facility accessibility and spatial coverage metrics (U_3).
- Personnel verification: Active RF identification (RFID) tags (2.4 GHz) were used by certified caregivers. Directional readers captured unique 64-bit electronic product code strings upon entry/exit events, transmitting through the recommended standard 485 serial bus. The identification accuracy was 98%, enabling precise caregiver density tracking.
- Facility occupancy: Piezoresistive thick-film force sensors were embedded in nursing beds to generate an analog voltage proportional to mechanical strain. Local analog-to-digital converters were used to collect signals at 10 Hz. A binary threshold ($\geq$ 15 kg) registered

steady-state occupancy with 99% accuracy, converting physical presence into nursing bed ratios.

- Flow assessment: Dual-beam passive infrared sensors were mounted at community thresholds to produce transistor-transistor logic pulses upon consecutive beam interruptions. Hourly aggregation (95% accuracy) was conducted to quantify facility traffic volumes, reflecting high-end service utilization.
- Service authentication: Near field communication readers (13.56 MHz) were used to verify government-supported elderly care services. Passive International Organization For Standardization/International Electrotechnical Commission 1444314443 tags were used to secure handshakes with 0.3 s latency, generating timestamp logs compiled into service supply efficiency metrics (U_1).

The collected sensor data were aggregated into normalized time-series matrices. The datasets were fused with municipal records, white papers, and industrial databases from the Liaoning Statistical Yearbook.[5] Sensors were regularly calibrated to mitigate sensor drift. Data anomalies were detected using the 3σ principle, and outliers caused by electromagnetic interference or network instability were removed.[12] Linear interpolation was adopted to reduce transmission loss to less than 5%. The ages of 42.1% of the elderly were between 60 and 69 years, 38.4% between 70 and 79 years, and 19.5% aged older than 80 years. In terms of educational attainment, 31.2% had completed primary school or lower, 52.3% had attained secondary school education, and 16.5% had received higher education. Financially, 28.7% were classified as low-income individuals, 58.5% as middle-income individuals, and 12.8% as high-income individuals.[13]

2.3 Data synchronization

A challenge in governance-oriented sensing networks lies in the structural heterogeneity of data streams. The deployed sensors operate under divergent temporal frequencies and activation mechanisms. GPS is used to capture spatial accessibility at discrete intervals, RFID to generate event-driven personnel mobility logs, pressure sensors to deliver continuous high-frequency voltage fluctuations from nursing beds, and infrared counters to record intermittent stochastic crossings. By inputting asynchronous data into an LSTMDNN model, temporal misalignment must be corrected for recurrent sequence learning.

Therefore, we implemented a two-stage temporal synchronization and data fusion protocol before model training. First, irregular sampling rates and intermittent connectivity, which are common in industrial networks, were mitigated using forward-fill imputation combined with linear interpolation. This ensured the continuity of missing fragments, maintaining a cumulative loss rate of less than 5%. Second, a uniform temporal bucket-aggregation scheme was applied to project multimodal streams into a synchronized grid.

Continuous and event-driven signals were downsampled or aggregated into standardized epoch intervals (Δt), aligned with the three-year macro-evaluation cycle through daily and monthly mean vectors. For high-frequency fluctuations (bed pressure readings used to infer binary occupancy), a rolling median filter with a window size was applied to suppress transient electromagnetic noise as follows.

$$\tilde{P}_t = \text{median}\left(P_{t-w},\ldots,P_t\right) \tag{1}$$

Here, $\tilde{P}_t$ is the filtered/calibrated signal value, representing the smoothed, noise-reduced sensor value calculated at the specific time step t, P_{t-w} is the historical boundary value recorded at w time steps relative to t, and P_t is the current raw signal value. At every t, the system collects the current measurement and the previous measurement at w, finds their median, and outputs P_t, effectively removing high-frequency noise spikes and preserving the sharp, authentic transitions in physical events (such as a patient shifting weight on a pressure-sensitive nursing bed).

Radio frequency identification (RFID)/near field communication (NFC) transaction data were integrated over the target epoch to yield continuous density values. The resulting time-aligned matrix was subsequently reduced by using principal component analysis into five principal components, capturing 96.3% of the total variance. This ensured perfectly synchronous time-series vectors for the LSTM input layer. By applying real-time physical telemetry to latent policy dynamics, the reliability of governance-oriented sequence modeling is enhanced.[14]

2.4 LSTM-DNN model

A hybrid deep learning model was constructed using LSTM for temporal feature extraction and DNN for capturing high-order nonlinear interactions between system indicators.[15] To align the model with the regional cycle, a dynamic time window (three years) was used. For the evaluation of the model's performance, a CCD model was employed. We introduced a coordination adjustment factor (λ) to quantify the feedback effect of the coordination level (U) on the raw coupling intensity. The modified coupling degree (C) is calculated as

$$C = \sqrt[3]{\frac{U_1 \times U_2 \times U_3}{\left(\left(U_1 + U_2 + U_3\right)/3\right)^3}} \times \left(1 + \lambda U_3\right). \tag{2}$$

Here, U_1 represents the development score of PECS, U_2 represents the ECI score, and U_3 represents the coordination score. λ was optimized to 0.2 on the basis of the grid search method to reflect the synergistic contribution of regional integration.

The comprehensive development index (T) and the final coupling coordination degree (D) are defined as

$$T = \alpha U_1 + \beta U_2 + \gamma U_3, \tag{3}$$

$$D = \sqrt{C \cdot T}. \tag{4}$$

Here, $\alpha = 0.35$, $\beta = 0.40$, and $\gamma = 0.25$ were determined by the entropy weight method to balance the contribution of each system.

The model was evaluated using a 22-indicator system categorized into three layers: PECS development, ECI development, and the coordination level (Tables 1 and 2). The indicator system was constructed to assign specific sensor modalities to verify soft statistical data with hard physical measurements.

2.5 Model training and validation

The model was trained using a standardized dataset where all variables were processed to a scale of [0,1] using Min-Max normalization. To prevent overfitting and manage the high dimensionality of the 22 indicators, principal component analysis was conducted. As a result, the input space was reduced to five principal components with a cumulative variance of 96.3%. Training was conducted with fivefold cross-validation. Robustness was verified by varying the weight coefficients and replacing statistical data with exclusively sensor-derived datasets to test for consistency. The predictive performance was evaluated using root mean square error (*RMSE*), mean absolute error (*MAE*), and the coefficient of determination (R^2). The model's generalization ability was validated by comparing it with that of different industrial transition regions. This sensor-to-model method enabled an assessment of how technological innovation in ECI affected the coordination of the elderly care system.

3. Results

The optimization of the coordination adjustment factor (λ) is critical for balancing the contribution of the three subsystems. A grid search was conducted to evaluate the impact of λ on the model's error. The results indicate a parabolic trend in *RMSE*, where the model showed its peak predictive accuracy at $\lambda = 0.2$, yielding a minimum *RMSE* of 0.029 (Fig. 1). Deviations from this optimal value lead to increased error. Data with a lower λ fail to account for the synergistic effects of coordination, whereas data with a higher value over-sensitize the model to coordination volatility, leading to higher variance in prediction.

Table 1
Sensor-integrated indicator system for elderly care coordination.

System layer	Criterion layer	Indicator layer	Sensor (network)	Specification
PECS	Security capacity	Facility coverage	GPS	Error of less than 5 m
		Nursing bed ratio	Pressure	Accuracy of 99%
	Supply efficiency	Caregiver density	RFID	Accuracy of 98%
		Service efficiency	NFC	Latency of 0.3 s
ECI	Scale and vitality	Innovation rate	IoT	Usage frequency log
		High-end service	Infrared	Counting accuracy of 95%
Coordination	Resource sharing	Platform utilization	Network	Access frequency
	Interaction	Talent mobility	RFID/GPS	Mobility trajectory
	Demand matching	Supply-demand index	Satisfaction	Likert scale (1–5)
	Spatial balance	Operational efficiency	IoT	Active service hours

Table 2
Sensor-integrated indicators.

System layer	Criterion layer	Indicator	Description
PECS	Basic security capacity	Policy completeness	Number of provincial-level elderly care policies
		Elderly care facility coverage	(Urban + rural facilities)/total communities × 100%
		Proportion of nursing beds	Nursing bed count/total bed count × 100%
	Social security level	Basic pension insurance participation rate	Insured population/eligible population × 100%
		Per capita pension level	Monthly average pension amount
	Service supply efficiency	Professional caregiver density	Certified caregivers/elderly population (per 1,000 elderly)
		Government purchased service efficiency	Beneficiary elderly/target population × 100%
ECI	Industrial scale and vitality	ECI contribution to GDP	ECI added value/gdp × 100%
		ECI enterprise growth rate	(Current enterprises - previous enterprises)/previous enterprises × 100%
		ECI investment growth rate	(Current investment - previous investment)/previous investment × 100%
	Innovation and structure	Service and product innovation	(New patents + new services)/ total enterprises
		High-end health care service proportion	High-end service revenue/total ECI revenue × 100%
		Technology conversion rate	Industrialized projects/ approved projects × 100%
Coordination	Resource sharing efficiency	Integration of medical and elderly care coverage	Qualified medical-elderly care institutions/total institutions × 100%
		Resource sharing platform utilization rate	Active users/registered users × 100%
		Cross-departmental policy coordination	Joint policies/total policies × 100%
	Factor flow and interaction	Talent mutual recognition rate	Interchangeable positions/total professional positions × 100%
		Industrial feedback fund proportion	Enterprise donations/public pecs expenditure × 100%
	Demand matching and response	Service supply-demand matching index	Matching degree between elderly demand and supply
		Policy response speed	Time lag between national policy and local implementation
	Spatial coordination	Urban-rural resource balance index	(Rural per capita investment/ urban per capita investment) × (rural facility coverage/urban facility coverage)
		Regional coordination project proportion	Cross-city project investment/ total investment ×100%

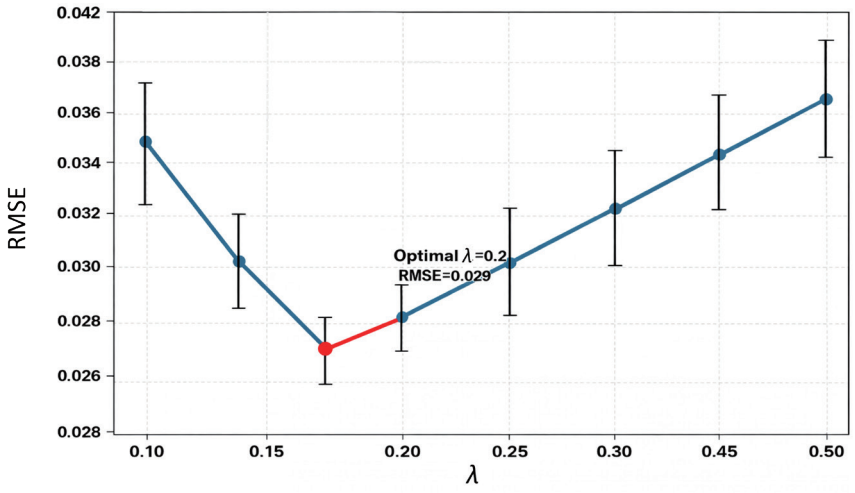

Fig. 1. (Color online) Optimization of coordination adjustment factor (λ) relative to *RMSE* for sensor-integrated LSTM-DNN model.

Sensor data are integrated for fidelity evaluation. The ablation study results showed that the sensor-integrated LSTM-DNN model significantly outperformed other models, achieving an R^2 of 0.923 and reducing *RMSE* by 29.3% (Table 3). This result is attributed to the execution of the multi-sensor temporal synchronization protocol. In deep learning models, feeding raw, asynchronous multi-sensor data used by recurrent models induces gradient instability and error propagation due to fractured time steps. By establishing a uniform temporal bucket-aggregation grid, the alignment step effectively preserved sequence fidelity and stabilized hidden state transitions across the three-year dynamic windows. Consequently, the LSTM-DNN model without sensor data performs reasonably well (R^2 = 0.902), but lacks the structural calibration provided by the synchronized sensing layer.

The calculated CCD for Liaoning Province of China from 2018 to 2023 demonstrated a steady transition from barely coordinated to moderately coordinated levels (Table 4).

The final coordination degree (D) increased from 0.54 to 0.79 over the six years. This growth was increased by consistent improvements in PECS (U_1) and ECI (U_2), which increased from 0.32 to 0.52 and 0.26 to 0.51, respectively. The modified coupling degree (C) reached 0.96 by 2023, suggesting that the public and market sectors were highly interdependent, although the final coordination level (D) was constrained by the slower growth of the coordination mechanism (U_3).

The coordination trajectory was categorized into three phases. During the preliminary run-in stage (2018–2019), growth was slow (from 0.54 to 0.58) owing to fragmented policy implementation and a lack of market vitality. In the policy-driven stage (2020–2021), rapid improvement (from 0.58 to 0.68) was observed, where sensor data contributed to a 15% increase in the elderly care medical service following the implementation of national aging response strategies. In the system optimization stage (2022–2023), steady advancement (from 0.68 to 0.79)

Table 3
Model performance comparison.

Model	*RMSE*	*MAE*	R^2
Traditional CCD model	0.041	0.035	0.872
LSTM	0.038	0.031	0.891
LSTM-DNN (without sensor data)	0.034	0.028	0.902
Sensor-integrated LSTM-DNN (this study)	0.029	0.024	0.923

Table 4
CCD of Liaoning Province of China (2018–2023).

Year	PECS (U_1)	ECI (U_2)	Coordination (U_3)	Modified coupling degree (C)	Final coordination degree (D)	Coordination level
2018	0.32	0.26	0.18	0.82	0.54	Barely coordinated
2019	0.35	0.29	0.20	0.84	0.58	
2020	0.39	0.33	0.25	0.87	0.63	Primary coordinated
2021	0.43	0.38	0.32	0.90	0.68	
2022	0.47	0.44	0.38	0.93	0.74	Moderately coordinated
2023	0.52	0.51	0.43	0.96	0.79	

was observed, characterized by improved healthcare resource allocation efficiency and tech-driven industrial innovation.

Despite the increasing trend, significant health-oriented constraints persist. The urban-rural resource imbalance remains the primary bottleneck; sensor-verified data show that rural per capita elderly care investment is only 43% of urban levels, which reduces the overall CCD by approximately 0.05. Furthermore, a time lag in policy implementation of 1.2 years prevents real-time responsiveness to elderly health needs. Policy coordination and healthcare-related innovation are the most effective levers for improving coordination.

Comparisons with domestic and international data highlighted structural differences. Liaoning's CCD remained 0.15 lower than that of Hangzhou, owing to a deficit in high-end healthcare services (12% in Liaoning and 28% in Hangzhou). When compared with the Ruhr Region in Germany (a 35% involvement) or Kitakyushu in Japan (30%), Liaoning's social organization involvement was significantly lower at 17%. This result reflects the lingering unit endowment of China's old industrial transition regions, where elderly care has been provided by state-owned enterprises rather than social or private ones.

4. Discussion

Sensor technology facilitates the transition from ambient sensing, which is restricted to localized and immediate responses, to governance sensing, where sensor networks are used in feedback loops for macro-system coordination.[9] The results of this study show that coordination failures in industrial transition regions are mainly attributable to deficiencies in data fidelity, and a standardized, sensor-integrated evaluation model ensures the real-time visibility of complex social systems. The 29.3% reduction in *RMSE* in the ablation study result indicates that sensor data can be used to effectively correct the inherent biases and temporal delays associated with

traditional statistical datasets. The sensing layer is proven to be a critical infrastructure component for evidence-based healthcare coordination.

The results also highlight the importance of sensor durability and reliability in sustaining healthcare coordination systems. Narrowband IoT and low-power wide-area network protocols are necessary to ensure consistent long-distance data transmission from rural areas, preserving the battery life of wearable and embedded devices. For a stable regional CCD model, sensors must maintain calibration fidelity even under unstable operating conditions.[10] Although linear calibration procedures have presented robust steady-state performance in laboratory environments (R^2 = 0.95), challenges remain in the deployment of the developed model in industrial transition regions. Electromagnetic interference, structural vibrations, and voltage fluctuations can induce nonlinear drift and stochastic noise spikes. To mitigate such drifts and noise, discrete Kalman filtering must be adopted to enable the estimation of physical states by recursively balancing measurement uncertainty against analytical process models.[G3] For long-term deployments subject to material aging or temperature-induced sensitivity changes, adaptive drift correction algorithms must also be implemented to automatically recalibrate baseline voltage thresholds during zero-occupancy periods, thereby sustaining data fidelity without manual intervention.[16]

The analysis results of coordination levels (U_3) show that isolated, single-scenario sensors, such as infrared counters, are insufficient for capturing high-fidelity data required for healthcare quality evaluation. To address this insufficiency, next-generation multi-sensor systems are required to integrate physiological clinical monitoring, such as continuous blood pressure and glucose telemetry, with ambient behavioral sensing such as voice-activity and daily social-interaction data. Such systems must provide standardized data acquisition and cross-layer communication protocols for effective heterogeneous data integration.

Asynchronous timelines must be well managed when combining continuous, high-frequency medical telemetry with bursty, event-triggered behavioral metrics. Without standardized data, hardware-level timestamping, and unified sampling frequencies, the time alignment method cannot be applied appropriately. Rigorous data standardization enables deep learning models to evaluate long-term service impacts, allowing municipal health authorities to deploy targeted interventions well before critical medical emergencies occur.[17] Standardized data can also mitigate administrative coordination bottlenecks, reducing the risk of systemic public health failures.

By leveraging sensor data to identify regional coordination indicators, a standardized acquisition protocol tailored to multi-subject healthcare systems can be formulated for industrial transition regions. This protocol tackles the current lack of calibration and quality control standards in regional-scale IoT networks.[5] Sensor data integration into deep learning models enables the optimization of response latency and sampling frequency while simultaneously enhancing predictive accuracy for healthcare decision-making and governance.

In policy lag modeling, an administrative execution latency of 1.2 years was observed before macro-level interventions manifested as structural changes in elderly care networks. To reduce the latency, policy latency must be encoded as an explicit time-delay variable using the LSTM input vector.[18] By introducing a lagging shift operator to the policy input tensor, the recurrent

neural network can map delayed dependencies between regulatory revisions and their eventual impact on physical sensor metrics, such as caregiver density or facility occupancy.[18]

Overall, the results of this study prove that sensor-based data enable closed-loop governance, where real-time indicators such as facility utilization and emergency response timeliness guide efficient resource reallocations. For industrial transition regions, this model can be used to optimize healthcare outcomes for the elderly by employing low-cost sensing technologies to overcome the historical silos of fragmented administrative statistics, creating a responsive and technologically integrated healthcare ecosystem. Although empirical validation was restricted to 14 prefecture-level cities in Liaoning Province, the developed model can be applied to other heavy-industrial transition zones experiencing similar demographic decline and economic restructuring. The model can be deployed in neighboring rust-belt regions such as Heilongjiang Province or resource-dependent economies such as Shanxi Province.[19] When transferring the model, the modified CCD equations and LSTM temporal sequence blocks can be used. By updating the data input layer with localized socioeconomic baseline data obtained from regional statistical yearbooks and calibrating edge sensing thresholds, municipal infrastructure can be aligned with the demands for elderly health care.[19]

5. Conclusion

By introducing a health-oriented quadruple subject coordination framework (government–market–family–unit) and an advanced sensor-integrated LSTM–DNN evaluation model, elderly healthcare coordination outcomes are quantified across industrial transition regions of Liaoning Province, China. The developed model showed steady structural progress in the regional CCD, which increased from 0.54 in 2018 to 0.79 in 2023. The model captured an initial run-in stage characterized by fragmented policy implementation, a policy-driven acceleration phase that expanded medical coverage, and a system optimization stage propelled by industrial innovation and refined resource allocation. The developed model applies low-level sensor data to macroscopic administrative logic. By feeding synchronized, noise-filtered multi-sensor datasets, derived from GNSS, RFID, piezoresistive force, PIR, and NFC arrays, into the hybrid recurrent neural network, the model eliminated gradient instabilities caused by fractured time steps. As a result, the sensor-integrated architecture outperformed other models, reducing predictive error (*RMSE*) by 29.3% and achieving $R^2 = 0.923$.

Despite these advances, persistent bottlenecks remain, including acute urban–rural resource imbalances, a 1.2-year policy implementation latency, and limited private or social sector involvement linked to the unit-endowment legacy of industrial bases. To enhance applicability, policy latency was encoded as a quantitative time-delay input in the LSTM layer. Discrete Kalman filtering and adaptive drift correction must be introduced to maintain calibrated statuses against industrial noise and material degradation. The model can be used for other industrial regions, providing an objective, responsive, and technologically integrated foundation for next-generation public healthcare management on the basis of a standardized data acquisition and synchronization template.

Acknowledgments

This research was supported by the 2025 Shenyang Philosophy and Social Sciences Planning Project (Project No. SY202557Y).

References

1 China Year Books: https://www.chinayearbooks.com/tag/liaoning-statistical-yearbook (accessed April, 2026).
2 H. Broyles, N. R. Sperber, C. I. Voils, R. T. Konetzka, N. B. Coe, and C. H. Van Houtven: Med. Care Res. Rev. **73** (2015) 349. https://doi.org/10.1177/1077558715614480
3 J. Offer: Front. Sociol. **8** (2023) 1076750. https://doi.org/10.3389/fsoc.2023.1076750
4 Y. Li, Z. Zhang, and X. Gao: Sustainability **14** (2022) 6790. https://doi.org/10.3390/su14116790
5 L. Guo, H. K. Lee, S. Oh, G. R. Koirala, and T.-i. Kim: ACS Sens. **10** (2025) 3239. https://doi.org/10.1021/acssensors.5c00024
6 M. I. Jordan and T. M. Mitchell: Science **349** (2015) 255. https://doi.org/10.1126/science.aaa8415
7 J. Liu and B. Wang: Sustainability **17** (2025) 11357. https://doi.org/10.3390/su172411357
8 B. Zieni, M. A. Ritchie, A. M. Mandalari, and F. Boem: Sensors **25** (2025) 853. https://doi.org/10.3390/s25030853
9 J.-M. Lepioufle, P. Schneider, P. D. Hamer, R. Å. Ødegård, I. Vallejo, T. V. Cao, A. Taherkordi, and M. Wojcikowski: Env. Data Sci. **3** (2024) e19. https://doi.org/10.1017/eds.2024.18
10 E. Achirei and L. Alboaie: Procedia Comput. Sci. **246** (2024) 2274. https://doi.org/10.1016/j.procs.2024.09.564
11 L. Wang, S. Zhou, and J. Qian: Inf. Fusion **126** (2026) 103670. https://doi.org/10.1016/j.inffus.2025.103670
12 M. Z. Uddin, W. Khaksar, and J. Torresen: Sensors **18** (2018) 2027. https://doi.org/10.3390/s18072027
13 M. Koo and S.-W. Yang: Encyclopedia **5** (2025) 18. https://doi.org/10.3390/encyclopedia5010018
14 Y. Bai, X. Xue, T. Su, X. Jin, and J. Kong: J. Ocean Eng. Sci. In press (2026). https://doi.org/10.1016/j.joes.2026.04.013
15 K. Chen, D. Zhang, L. Yao, B. Guo, Z. Yu, and Y. Liu: ACM. Comput. Surv. **54** (2021) 1. https://doi.org/10.1145/3447744
16 M. Wang, X. Dong, C. Qin, and J. Liu: Measurement **167** (2021) 108170. https://doi.org/10.1016/j.measurement.2020.108170
17 C. Rathnayake, W. Chen, S. Jayawickrama, and D. Lai: Sensors **26** (2026) 3477. https://doi.org/10.3390/s26113477
18 Z. Y. Tan, J. M.-Y. Lim, C. R. Sarimuthu, and R. Mukhopadhyay: Public Transp. (2026). https://doi.org/10.1007/s12469-025-00419-5
19 X. Liu, L. Tu, and B. Zhou: Sustainability **18** (2026) 4314. https://doi.org/10.3390/su18094314